Progress In Electromagnetics Research, Vol. 128, 91–103, 2012

MULTI-REFRACTION WITH SAME POLARIZATION STATE IN TWO DIMENSIONAL TRIANGULAR PHOTONIC CRYSTALS

G. Dong[1], J. Zhou[1,*], X. Yang[2], and X. Meng[2]

[1]State Key Lab of New Ceramics and Fine Processing, Department of Materials Science and Engineering, Tsinghua University, Beijing 100084, China

[2]Department of Optics, Shandong University, Jinan 250100, China

Abstract—Multi-refraction effects with one polarization in a two-dimensional triangular photonic crystal (PhC) were systematically studied by theoretical analysis and numerical simulation. The more complicated refraction behaviors can be excited in the higher band regions based on the intricate undulation of one band or the overlap of different bands. A novel non-handedness effect is proposed for the first time with group velocity perpendicular to phase velocity. Furthermore, triple refraction phenomena and special collimation effects of symmetrical positive-negative refraction with the loose incident conditions have been found in different band regions of this PhC. These unique features will provide us with more understanding of electromagnetic wave propagation in PhCs and give important guideline for the design of new type optical devices.

1. INTRODUCTION

Photonic crystals are a class of periodically modulated dielectric materials, which can be applied to manipulate light at the wavelength scale [1–9]. More recently, negative refraction [10–12] in PhCs has attracted much attention for their potential application in many fields, such as focusing imaging [13–15], microcavity [16] and beam splitting [17–24]. In contrast to negative index materials (NIMs) [25–28] with simultaneous negative electrical permittivity and magnetic permeability, negative refraction in PhC is based on the special dispersion relations of photonic bands, instead of strong resonance

Received 3 April 2012, Accepted 7 May 2012, Scheduled 18 May 2012

* Corresponding author: Ji Zhou (zhouji@tsinghua.edu.cn).

mechanism, so the loss could be much smaller than the former. Beam splitting is one of important effects in the negative refraction of PhCs. Higher-order diffractions with different polarization states [17, 18, 24] and the incident beam with different wave vectors [19, 20] can be used to realize beam splitting. For the same polarization state, beam splitting based on the positive-negative refraction was first reported by Luo et al. in the square PhC [21]. Afterward, positive-negative refraction based on the overlap of the second and third bands in square PhCs has been studied by theoretical analysis and numerical simulations [22, 23]. However, up to now, the refraction effects of the higher bands in PhC have never been investigated systematically. Their remarkable properties are the main topic of our study here.

Compared with square PhCs, triangular PhCs display the better photonic band gap (PBG) properties and the more complex dispersion characteristics [29]. In this paper, by utilizing a 2D triangular lattice PhC, we analyze the necessary conditions of multi-refraction in PhC and demonstrate the possible multi-refraction behaviors at different frequencies. The plane-wave expansion method and the finite-difference time-domain (FDTD) method were used to calculate the band structure of PhC and simulate electromagnetic wave propagation with perfectly matched layer (PML) boundary conditions. Due to the desired conditions for the case under study, only the TM modes are considered here with electric field **E** parallel to the dielectric rods.

2. LATTICE AND BAND STRUCTURES

The lattice structure studied in this work is a 2D triangular PhC composed of connected hexagonal Si rods in air background with a refractive index of $n = 3.4$, as shown in Fig. 1(a), whose preparation method has been proposed in our previous work [30]. In order to avoid higher order Bragg diffractions out of the PhC, the condition of wave vector $\boldsymbol{k} \leq 0.5 \times 2\pi/a_s$ (where a_s is the surface lattice constant along the ΓK direction, here $a_s = a$) should be satisfied. Hence, the lowest seven bands for TM polarization are shown in Fig. 1(b) with the frequency normalized quantity of a/λ or $\omega a/2\pi c$ (a is the lattice constant), the inset represents the first Brillouin zone of triangular PhC with three high-symmetry lattice points, and the point Γ is the Brillouin zone center.

3. MULTI-REFRACTION IN A SINGLE BAND

According to the k-conservation relation in wave-vector diagram [31], two or more modes at the same frequency with different refractive

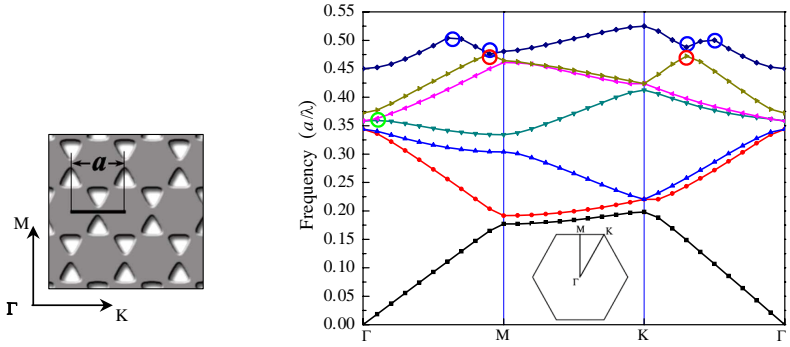

Figure 1. (a) Schematic of the 2D triangular lattice PhC with hexagonal dielectric rods in air; (b) Lowest seven band structures of this PhC for TM polarization.

behaviors need two or more equal frequency contours (EFCs) to validly intersect the k-conservation line, which means a single band should have at least one frequency up and down out of three given high-symmetry points. As identified with the circles in Fig. 1(b), the fourth, sixth and seventh bands of the PhC satisfy this condition of multi-refraction in a single band and should be the ideal candidates to induce multi-refraction effects.

3.1. Numerical Calculation and Analysis

In Fig. 1(b), the fourth band has one undulation circled by the green ring around the frequency of $\omega = 0.36a/\lambda$. In order to gain a clear idea of its refractive characteristic, the corresponding band surface and EFC plot in the first Brillion zone are shown in Fig. 2(a) with the red and blue to distinguish the different regions with high and low frequencies. Its band surface looks like six triangular peaks connected by six concave valleys around the center point Γ.

Figure 2(b) gives the wave vector diagram with the incident angle of $\theta_{inc} = 25°$ at the frequency of $\omega = 0.36a/\lambda$, where the blue circle represents the air EFC, the orange arrows denote the wave vectors $\boldsymbol{K}$, and the blue arrow denotes the group velocity vector in air. According to the k-conservation relation, the dashed line means the conservation of the parallel components of wave vectors which intersects the EFC of $0.36a/\lambda$ with two intersections at the points A and B. By the definition of group velocity $\boldsymbol{V}_{gr} = \nabla_k \omega$, the group velocity vector (i.e., energy vector) is always oriented perpendicular to the EFC in the frequency-

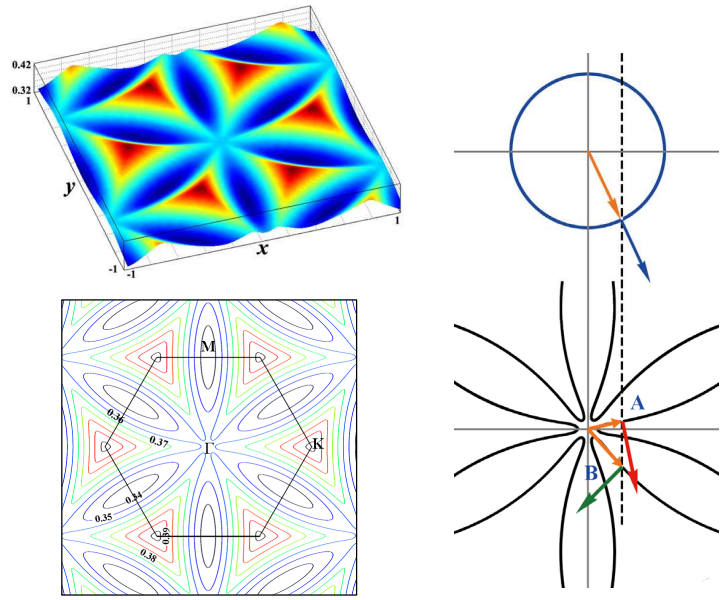

Figure 2. (a) Band surface and EFC plot of the fourth band; (b) Wave vector diagram at the frequency of $0.36a/\lambda$ with the incident angle of 25°.

increasing direction. The red and green arrows denote the directions of positive and negative group velocity vectors, respectively. The necessary condition for left-handed (LH) material is $\boldsymbol{K} \cdot \boldsymbol{V}_{gr} < 0$, which can be used to distinguish the left and right-handedness (RH) of EMW. However, in this case, the group velocity vectors of both positive and negative refracted beams are almost perpendicular to their wave vectors (i.e., phase velocity vector) with $\boldsymbol{K} \cdot \boldsymbol{V}_{gr} = 0$, which denote their rightness effects are hardly distinguished with non-handedness. Moreover, their refractive angles can be modulated within the scope from 10° to 35° for the positive refracted beam and the scope from −39° to −50° for the negative one by adjusting the incident angle from 5° to 50°. When $\theta_{inc} < 20°$, a third refracted beam with a large refractive angle will be excited by the third intersection between the k-conservation line and the EFC of the fourth band at $\omega = 0.36a/\lambda$.

Obviously, in Fig. 1(b), the sixth band has two undulations circled by the red rings. Its band surface with the hexangular volcanic vent surrounded by concavities at six corners and the corresponding EFC

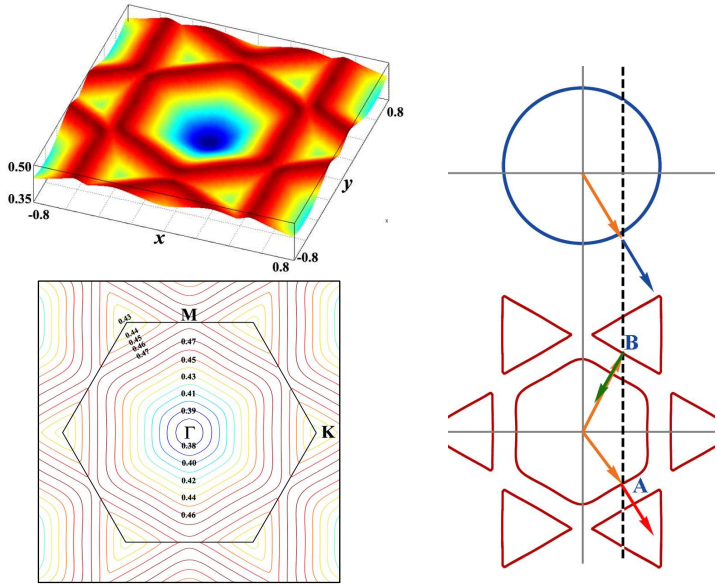

(a) (b)

Figure 3. (a) Band surface and EFC plot of the sixth band; (b) Wave vector diagram at the frequency of $0.46a/\lambda$ with $\theta_{inc} = 30°$.

plot are illustrated in Fig. 3(a). Within the frequency range from 0.44 to $0.47a/\lambda$, the PhC has dual parallel EFCs with opposite curvatures for the same frequency. With the frequency increasing, the inner EFC expands, whereas the outer shrinks gradually. As an example, when the working frequency is chosen to be $0.46a/\lambda$, the wave vector diagram with $\theta_{inc} = 30°$ is illustrated in Fig. 3(b). According to the definition of group velocity $\boldsymbol{V}_{gr}$, it is clear that the group velocity of the inner EFC points outward with $\boldsymbol{K} \cdot \boldsymbol{V}_{gr} > 0$ and the group velocity of the outer EFC points inward with $\boldsymbol{K} \cdot \boldsymbol{V}_{gr} < 0$. Hence, the LH− and RH+ refractive waves can be excited simultaneously at the same frequency. Due to the parallel inward and outward EFCs, the positive and negative refracted waves have the symmetrical refractive angles of $\pm 30°$ and their separating angle should be nearly stationary at 60° within a wide scope of incident angle.

The seventh band has more frequency undulations circled by the blue rings in Fig. 1(b). In Fig. 4(a), its band surface looks like an approximately round volcanic vent surrounded by six triangular peaks at six corners, and the corresponding EFC distribution is shown with the 0.01 step. It is clear that the more frequent undulations on the band

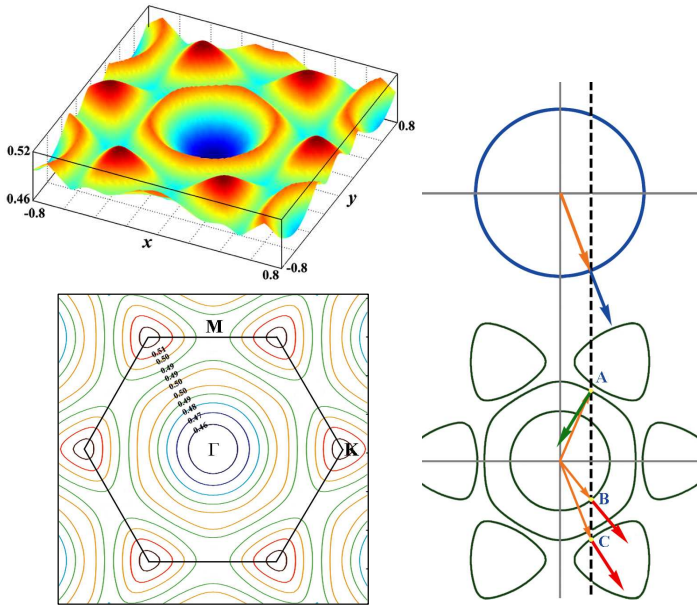

Figure 4. (a) Band surface and EFC plot of the seventh band; (b) Wave vector diagram at the frequency of $0.49a/\lambda$ with $\theta_{inc} = 20°$.

surface will lead to the more closed EFCs within the frequency scope from 0.488 to $0.50a/\lambda$. For instance, the wave vector diagram at the frequency of $0.49a/\lambda$ with $\theta_{inc} = 20°$ is illustrated in Fig. 4(b), where two EFCs surrounding the center point Γ have the almost opposite curvatures and intersect the k-conservation line at two valid points of A and B with the inward and outward group velocities respectively. Based on the sign of $\boldsymbol{K} \cdot \boldsymbol{V}_{gr}$, we know that the refracted wave excited at point A is LH− and the one excited at point B is RH+. Simultaneously, the k-conservation line also intersects the corner EFC of $\omega = 0.49a/\lambda$ at the third point C, which may excite the second RH+ refracted beam. Therefore, the more intricate triple refraction may be excited in the seventh band.

3.2. Numerical Simulation and Result Analysis

In order to verify the above analysis results, a continuous Gaussian wave source with the spatial width of $10a$ is located in front of the PhC slab with the thickness of 30 layers, which can be regard as a

plane wave. Fig. 5 shows the schematic diagram of positive-negative refraction with the source EMW incidenting at a certain incident angle θ_{inc} from air upon the surface of PhC slab cut along the ΓK direction.

When the source wave of $\omega = 0.36a/\lambda$ is incident at $\theta_{inc} = 25°$, the FDTD simulation of distribution pattern of electric field is shown in Fig. 6(a), where the black and yellow arrows denote the directions of energy transmission and phase velocity respectively, and two parallel outgoing waves indicate the separate transmitted waves originating from the same source wave. Obviously, the incident EMW is divided into negative and positive refracted waves with different refractive angles in the PhC slab with their wave fronts approximately paralleling to the direction of EMW propagation. Since the wave vectors are perpendicular to their wave fronts, the condition of $\boldsymbol{K} \cdot \boldsymbol{V}_{gr} = 0$ is satisfied in this case without evident rightness of LH or RH. The further simulation results show that the refractive angle can vary gradually with the changing of incident angle. When the source wave is incident at $\theta_{inc} = 13.3°$, as Fig. 6(b) shows, the spatial wavelength of refracted waves become greater than before due to the reduced wave vectors, and the third refracted beam with a large refractive angle is excited in the space of positive refraction.

For the sixth band, we choose the EMW of $\omega = 0.46a/\lambda$ as the wave source to incident upon the surface of PhC slab with $\theta_{inc} = 30°$. The simulation pattern of electric field is shown in Fig. 7(a) with the incident wave divided into the symmetrical positive and negative waves with a stationary separate angle of 60°. Its remarkable characteristic is that the change of incident angle within the limited range from 6° to 53° scarcely has any impact on the symmetrical refractive angles

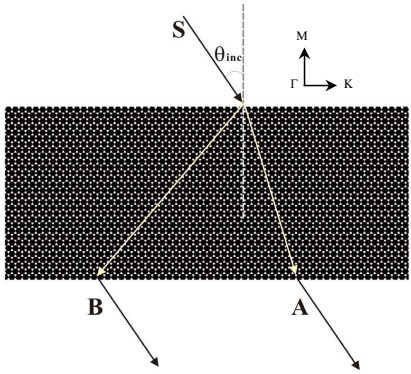

Figure 5. Diagram of EMW transmission from point S to points of A and B through the interfaces between air and the PhC slab.

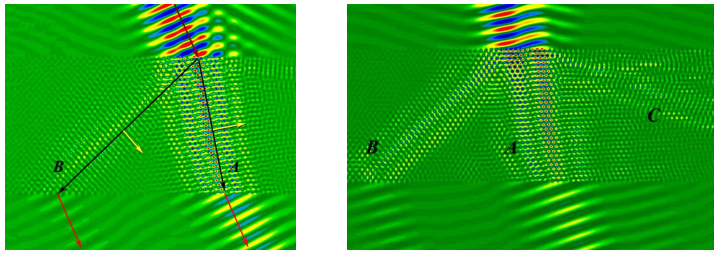

(a) (b)

Figure 6. The FDTD simulations of electric field distributions with (a) $\theta_{inc} = 25°$ and (b) $\theta_{inc} = 13.3°$ at the frequency of $0.36a/\lambda$ in the fourth band.

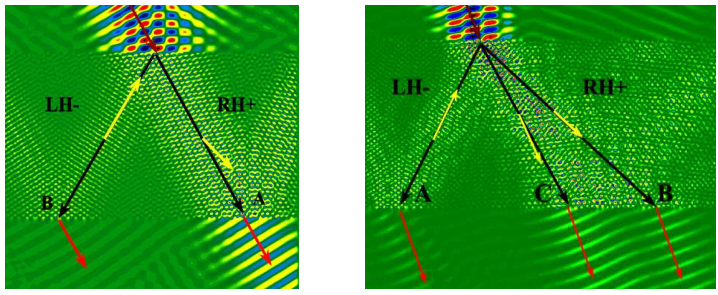

(a) (b)

Figure 7. The electric field distribution with the incident angle of (a) $\theta_{inc} = 30°$ at the frequency of $0.46a/\lambda$ and (b) $\theta_{inc} = 20°$ at the frequency of $0.49a/\lambda$.

due to the dual parallel EFCs with opposite curvatures at the same frequency. This unusual collimation effect of symmetrical positive-negative refraction may have a series of exciting potential applications, such as self-collimated beam splitter [32], spatial light modulator [33] and optical collimator [34].

Figure 7(b) shows the simulated electric field distribution in PhC slab with the incident EMW of $\omega = 0.49a/\lambda$ at the incident angle of 20°. It is clear that the incident EMW is split into negative and mixed positive refracted waves in this PhC slab with three separate parallel outgoing beams, which indicate there are two positive refracted waves in the positive space. This result well corresponds with the previous forecast of dual-positive and negative refractions for the seventh band.

The above results of numerical simulations agree well with the

previous theoretical analyzes, which demonstrate that the higher single band can excite the more complicate multi-refraction effects at the same frequency, such as non-handed refraction, collimation effect of symmetrical positive-negative refraction and triple refraction. They will provide significant potentials for the development of technological application.

4. MULTI-REFRACTION BASED ON OVERLAPPING BANDS

In the overlapping region of different bands, the PhC have two or more EFCs corresponding to different bands and each EFC yields one refracted beam, hence, more than one refractive mode will be excited at the same frequency. Based on this theory, the dual-negative refraction effect based on the overlapping of the second and third bands has been reported in our previous work [29]. In that case, the rightness effects of both two negative refractions are LH with $\boldsymbol{K} \cdot \boldsymbol{V}_{gr} < 0$.

It can clearly be seen in Fig. 1(b) that the fifth and sixth bands also overlap each other in a wide frequency region, which can be utilized to excite multi-refraction. The corresponding EFCs of the fifth band are shown in Fig. 8(a) with the six-pointed star contours surrounding the point Γ whose outward gradient will induce negative refraction. It can be seen from the EFCs of the sixth band in Fig. 3(b) that positive refraction can be excited in this PhC slab with the frequency less than $0.44a/\lambda$. In their overlapping region, the highlighted wave vector diagram of $0.42a/\lambda$ with $\theta_{inc} = 20°$ is shown in Fig. 8(a) to analyze the related rightness effects of two refracted waves. The analysis result

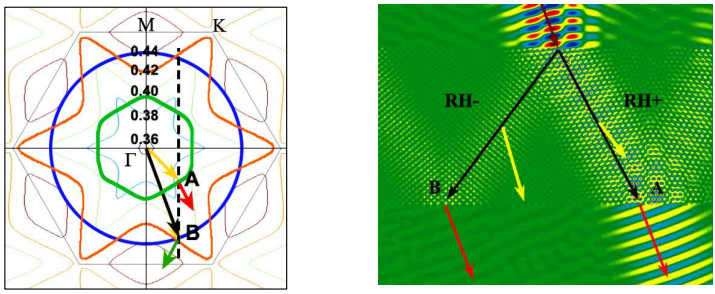

(a) (b)

Figure 8. (a) Wave vector diagram for the overlap of TM5 and TM6 bands; (b) Electric field distribution at the overlapping frequency of $0.42a/\lambda$ with $\theta_{inc} = 20°$.

shows that the sixth band can excite a RH+ refracted wave and the fifth band can excite a RH− refracted beam simultaneously. The simulation pattern has been shown in Fig. 8(b) to verify this analysis result. Just like the effect of positive-negative refraction in the sixth band, two symmetrical refracted waves with the collimation effect are re-excited at the frequency of $0.42a/\lambda$ based on the overlap of TM5 and TM6 bands.

5. CONCLUSION

In summary, we systematically investigated the multi-refraction effect of the higher bands in the 2D triangular PhC. The various multi-refractions have been found at different frequencies in the PhC. Two ways are utilized to realize the multi-refractions with one arising from a single band with intricate undulations and another resulting from the overlap of different bands. Furthermore, the relation between the refraction and the rightness effect has been investigated thoroughly. The unique features of non-handed refraction, collimation effect of symmetrical positive-negative refraction and triple refraction have been found in this work, which also can be extended to other PhC configurations. Since the PhC has more design flexibility, these characteristics of multi-refraction can be engineered easily with a large freedom. These original research results may bring important impact on electromagnetic transmission.

ACKNOWLEDGMENT

We gratefully acknowledge the financial support from National Natural Science Foundation (51102148, 90922025, 50922061, 51032003 and 60907005), Shandong Natural Science Foundation (ZR2010AM025 and ZR2011FQ011).

REFERENCES

1. Yablonovitch, E., "Inhibited spontaneous emission in solid-state physics and electronics," *Phys. Rev. Lett.*, Vol. 58, 2059, 1987.
2. John, S., "Strong localization of photons in certain disordered dielectric superlattices," *Phys. Rev. Lett.*, Vol. 58, 2486, 1987.
3. Wu, C. J., Y. C. Hsieh, and H. T. Hsu, "Tunable photonic band gap in a doped semiconductor photonic crystal in near infrared region," *Progress In Electromagnetics Research*, Vol. 114, 271–283, 2011.

4. Butt, H., Q. Dai, T. D. Wilkinson, and G. A. J. Amaratunga, "Photonic crystals & metamaterial filters based on 2D arrays of silicon nanopillars," *Progress In Electromagnetics Research*, Vol. 113, 179–194, 2011.
5. Hsu, H. T, T. W. Chang, T. J. Yang, B. H. Chu, and C. J. Wu, "Analysis of wave properties in photonic crystal narrowband filters with left-handed defect," *Journal of Electromagnetic Waves and Applications*, Vol. 24, No. 16, 2285–2298, 2010.
6. Li, H. and X. Yang, "Larger absolute band gaps in two-dimensional photonic crystals fabricated by a three-order-effect method," *Progress In Electromagnetics Research*, Vol. 108, 385–400, 2010.
7. Hung, H. C., C. J. Wu, T. J. Yang, and S. J. Chang, "Analysis of tunable multiple-filtering property in a photonic crystal containing strongly extrinsic semiconductor," *Journal of Electromagnetic Waves and Applications*, Vol. 25, No. 14–15, 2089–2099, 2011.
8. Lu, H, X. M. Liu, R. Zhou, D. Mao, and Y. Gong, "Tunable and robust reflection-free waveguides based on a gyromagnetic photonic crystal," *Journal of Electromagnetic Waves and Applications*, Vol. 25, No. 11–12, 1752–1761, 2011.
9. Dai, X., Y. Xiang, and S. Wen, "Broad Omnidirectional Reflector in the one-dimensional ternary photonic crystals containing superconductor," *Progress In Electromagnetics Research*, Vol. 120, 17–34, 2011.
10. Srivastava, R., S. Srivastava, and S. P. Ojha, "Negative refraction by photonic crystal," *Progress In Electromagnetics Research B*, Vol. 2, 15–26, 2008.
11. Liu, S. H. and L. X. Guo, "Negative refraction in an anisotropic metamaterial with a rotation angle between the principal axis and the planar interface," *Progress In Electromagnetics Research*, Vol. 115, 243–257, 2011.
12. Navarro-Cia, M., M. Beruete, F. J. Falcone, M. Sorolla Ayza, and I. Campillo, "Polarization-tunable negative or positive refraction in self-complementariness-based extraordinary transmission prism," *Progress In Electromagnetics Research*, Vol. 103, 101–114, 2010.
13. Martínez, A., H. Míguez, A. Griol, and J. Martí, "Experimental and theoretical analysis of the self-focusing of light by a photonic crystal lens," *Phys. Rev. B*, Vol. 69, 165119, 2004.
14. Ren, K., Z. Y. Li, X. B. Ren, S. Feng, B. Y. Cheng, and D. Z. Zhang, "Three-dimensional light focusing in inverse opal photonic crystals," *Phys. Rev. B*, Vol. 75, 115108, 2007.

15. Lu, M. H., C. Zhang, L. Feng, J. Zhao, Y. F. Chen, Y. W. Mao, J. Zi, Y. Y. Zhu, S. N. Zhu, and N. B. Ming, "Negative birefraction of acoustic waves in a sonic crystal," *Nature Material*, Vol. 6, 744–748, 2007.
16. Ruan, Z. and S. He, "Open cavity formed by a photonic crystal with negative effective index of refraction," *Opt. Lett.*, Vol. 30, 2308–2310, 2005.
17. Xiong, C., B. Zhang, X. Kang, T. Dai, and G. Zhang, "Diffracted transmission effects of GaN and polymer two-dimensional square-lattice photonic crystals," *Opt. Express*, Vol. 17, 23684–23689, 2009.
18. Balestreri, A., L. Andreani, and M. Agio, "Optical properties and diffraction effects in opal photonic crystals," *Phys. Rev. E*, Vol. 74, 036603, 2006.
19. Kim, A., K. B. Chung, and J. W. Wu, "Control of self-collimated Bloch waves by partially flat equifrequency contours in photonic crystals," *Appl. Phys. Lett.*, Vol. 89, 251120, 2006.
20. Wu, L. J., M. Mazilu, J. F. Gallet, T. F. Krauss, A. Jugessur, and R. M. de La Rue, "Planar photonic crystal polarization splitter," *Opt. Lett.*, Vol. 29, 1620, 2004.
21. Luo, Y., W. Zhang, Y. Huang, J. Zhao, and J. Peng, "Wide-angle beam splitting by use of positive-negative refraction in photonic crystals," *Opt. Lett.*, Vol. 29, 2920–2922, 2004.
22. Kang, X., G.-J. Li, and Y.-P. Li, "Positive-negative refraction effect based on overlapping bands in a two-dimensional photonic crystal," *J. Opt. Soc. Am. B*, Vol. 26, 010060, 2009.
23. Gajic, R., R. Meisels, F. Kuchar, and K. Hingerl, "Refraction and rightness in photonic crystals," *Opt. Express*, Vol. 13, 8596–8605, 2005.
24. Shi, Y., "A compact polarization beam splitter based on a multimode photonic crystal waveguide with an internal photonic crystal section," *Progress In Electromagnetics Research*, Vol. 103, 393–401, 2010.
25. Li, J., F. Q. Yang, and J. F. Dong, "Design and simulation of L-shaped chiral negative index structure," *Progress In Electromagnetics Research*, Vol. 116, 395–408, 2011.
26. Wu, Z., B. Q. Zeng, and S. Zhong, "A double-layer chiral metamaterial with negative index," *Journal of Electromagnetic Waves and Applications*, Vol. 24, No. 7, 983–992, 2010.
27. Kinto-Ramírez, H., M. A. Palomino-Ovando, and F. Ramos-Mendieta, "Photonic modes in dispersive and lossy superlattices

containing negative-index materials" *Progress In Electromagnetics Research B*, Vol. 35, 133–149, 2011.

28. Zhao, Y., F. Chen, H. Chen, N. Li, Q. Shen, and L. Zhang, "The microstructure design optimization of negative index metamaterials using genetic algorithm," *Progress In Electromagnetics Research Letters*, Vol. 22, 95–108, 2011.
29. Dong, G. Y., J. Zhou, X. L. Yang, and L. Z. Cai, "Dual-negative refraction in photonic crystals with hexagonal lattices," *Opt. Express*, Vol. 19, 12119, 2011.
30. Dong, G. Y., X. L. Yang, and L. Z. Cai, "Anomalous refractive effects in honeycomb lattice photonic crystals formed by holographic lithography," *Opt. Express*, Vol. 18, 16302–16308, 2010.
31. Leminger, O., "Wave-vector diagrams for two-dimensional photonic crystals," *Opt. Quantum Electro.*, Vol. 34, 435–443, 2002.
32. Yu, X. and S. Fan, "Bends and splitters for self-collimated beams in photonic crystals," *Appl. Phys. Lett.*, Vol. 83, 3251–3253, 2003.
33. Liu, L., S. L. Zheng, X. M. Zhang, X. F. Jin, and H. Chi, "Performance improvement of phase modulation with interferometric detection through low-biasing," *Journal of Electromagnetic Waves and Applications*, Vol. 24, No. 1, 123–132, 2010.
34. Xu, O., "Collimation lens design using Al-Ga technique for Gaussian radiators with arbitrary aperture field distribution," *Journal of Electromagnetic Waves and Applications*, Vol. 25, No. 5–6, 743–754, 2011.